Biochimica et Biophysica Acta, 1107 (1992) 77–85

BBAMEM 75644

Low-temperature phase behaviour of the major plant leaf lipid monogalactosyldiacylglycerol

Peter W. Sanderson and W. Patrick Williams

Biomolecular Sciences Division, King's College London, London (UK)

(Received 6 September 1991)

Key words: Galactolipid; Monogalactosyldiacylglycerol; DSC; Lipid phase behavior; X-ray diffraction; Freeze-fracture

Heating and cooling thermograms of unsaturated MGDG samples isolated from the leaves of *Vicia faba* are surprisingly featureless. This reflects the low enthalpies associated with phase transitions in highly unsaturated lipids and the fact that these transitions, in the case of MGDG, are to a large extent masked by those associated with the freezing and melting of ice. Careful choice of thermal heating/cooling regimes, combined with the use of real-time X-ray diffraction and freeze-fracture measurements, permits a detailed analysis of the phase behaviour of the system. The phase behaviour of unsaturated MGDG samples is shown to be basically similar to that seen in saturated MGDG samples. The lipid which exists in the inverted hexagonal (Hex_{II}) liquid crystal phase at room temperature forms a highly disordered lamellar gel (L_β) phase on cooling to temperatures below about −15°C. On reheating, this first reorganises at a temperature of about −10°C to form a well-defined L_{c1} phase. Above about −2°C, this melts to re-form the Hex_{II} phase. Samples re-cooled from temperatures between −2°C and 14°C revert directly to the L_{c1} phase while samples cooled from higher temperatures form the L_β phase. This reflects the fact that the former samples contain small amounts of unmelted L_{c1} phase lipid. The implications of these observations are discussed in terms of the general problems associated with the measurement of low-temperature phase behaviour of membrane lipids.

Introduction

Study of the phase behaviour of the sugar-containing glycolipids, common in plant and bacterial membranes, has tended to lag behind corresponding studies on the phospholipids which dominate the composition of animal cell membranes. While there has been a recent upsurge of interest in the properties of glucosyldiacylglycerols of the type found in bacteria [1–4], much less attention has been paid to the phase behaviour of the closely related galactolipids which dominate plant membrane lipid composition.

The phase behavior of the galactolipid monogalactosyldiacylglycerol (MGDG) is of special interest in that it is the major membrane lipid found in photosynthetic membranes of higher plants [5]. It is a non-bilayer forming lipid which normally hydrates to form into cylindrical inverted micelles that pack in a hexagonal lattice giving rise to the inverted hexagonal, or Hex_{II}, phase at room temperature [6]. At lower temperatures, this transforms to a lamellar phase. In the case of the C_{16} and C_{18} homologues found in biological membranes, at least, the lipid transforms directly to the lamellar gel (L_β) phase rather than via a lamellar liquid crystalline (L_α) phase [7]. In its native form MGDG is usually highly unsaturated. The main fatty acid substituents in the chloroplast membranes of higher plants are linolenic (18:3) and linoleic (18:2) acids [5]. The majority of the published studies on the phase behaviour of MGDG have, however, been carried out using fully-saturated lipids obtained by hydrogenation [7–9] or highly saturated lipids isolated from thermophilic cyanobacteria [10,11]. Shipley et al. [6] have performed X-ray diffraction studies on unsaturated MGDG isolated from *Pelagonium* but these studies were almost entirely restricted to measurements above 0°C where the lipid was in the Hex_{II} phase. A value of −30°C was cited for the gel-to-liquid crystal phase transition temperature but no data were presented to support this value.

In this study a range of physical techniques are used to investigate the phase behaviour of unsaturated MGDG isolated from the leaf tissue of *Vicia faba*. The phase behaviour of this lipid is shown to be more complex than is generally appreciated. The results ob-

Correspondence: W.P. Williams, Biomolecular Sciences Division, King's College London, Campden Hill, London W8 7AH, UK.
Abbreviations: MGDG, monogalactosyldiacylglycerol; L_α, liquid-crystal lamellar phase; L_β, gel lamellar phase; Hex_{II}, inverted hexagonal phase; L_c, crystal (sub-gel) lamellar phase.

tained raise a number of interesting questions regarding the factors governing the measurement of lipid phase transitions at temperatures below the freezing point of water.

Materials and Methods

Monogalactosyldiacylglycerol isolated from the leaves of *Vicia faba* (broad bean) was purchased from Lipid Products (Redhill, UK) and stored in chloroform/methanol (2:1, v/v) under nitrogen at −70°C. Gas chromatography and TLC measurements were performed as described elsewhere [12,13]. The acyl chain composition was 84% by weight linolenic acid (18:3), 5% linoleic acid (18:2), 2% oleic acid (18:1), 4% stearic acid (18:0) and 5% palmitic acid (16:0). These values are in reasonably good agreement with those reported in earlier studies performed on *Vicia faba* MGDG [12,13]. The lipid showed only a single spot when subjected to TLC. As lipid extracted from the TLC plates yielded identical thermograms to those of the lipid as purchased, the purchased material was used without further purification.

Differential scanning calorimetry (DSC). Samples were prepared by drying the lipid using a vacuum dessicator and then hydrating it with distilled water in a ratio of 1:2 lipid/water by weight so that water was present in excess. Care was taken to avoid lipid oxidation. Heating and cooling scans were performed with a Perkin-Elmer DSC-2 (Perkin-Elmer Ltd., Bucks., UK) fitted with a sub-ambient accessory. Temperature calibration was achieved using indium and dodecane standards and enthalpy calibration using indium. Transition temperatures were taken to be the intercept of the tangent of the rising peak slope with the baseline. A scanning rate of 5 C°/min was employed. Control TLC measurements showed no appreciable degradation of the lipids during the course of the measurements.

X-ray diffraction. Real-time X-ray diffraction was conducted at station 8.2 of the Daresbury Synchrotron Radiation Source. The samples, prepared as described above, were mounted in the X-ray beam between mica sheets in a modified Linkam THM600 temperature-controlled microscope stage (Linkam Scientific instruments, Surrey, UK). A monochromatic X-ray beam (0.15 nm) was used and the diffraction pattern detected by a quadrant detector. The samples were subjected to controlled heating and cooling scans at rates of 5 C°/min between defined temperature limits. The data collection system allowed 255 diffraction patterns to be collected consecutively with a 10 μs wait-time between patterns. The exposure time for each pattern was 4 s.

Freeze-fracture. Samples were mounted in a temperature-controlled environment chamber constructed in this laboratory which allowed cooling and heating between 20°C and −50°C at rates approximating to 5 C°/min before plunge quenching in nitrogen slurry. The samples were fractured and shadowed at −150°C in a Polaron freeze-fracture unit (Bio-Rad, UK).

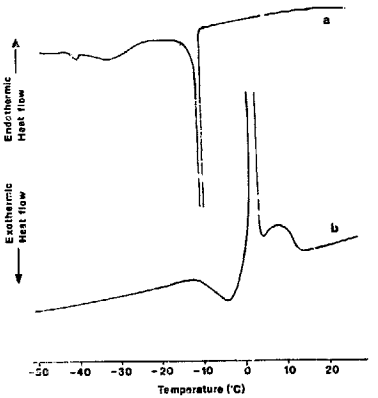

Fig. 1. Typical thermograms of an unsaturated MGDG sample cycled between −50°C and 20°C at a rate of 5 C°/min (a) cooling scan and (b) heating scan.

Results

Differential scanning calorimetry

Typical thermograms obtained for MGDG on heating and cooling between 20°C and −50°C are displayed in Fig. 1. The thermograms are surprisingly featureless when compared to the heating and cooling thermograms obtained with saturated MGDG samples [7].

On cooling from 20°C, a large exotherm is observed at around −10°C as illustrated in Fig. 1a. It, however, merely reflects the freezing of supercooled water in the sample. The degree of supercooling varied in different scans but freezing usually took place at a temperature between −10°C and −18°C. A much smaller broad exotherm, corresponding to a molar enthalpy of approximately 1.0 kcal/mol, centered at about −30°C together with a sharper exotherm centred at about −40°C is observed at lower temperatures. Samples cooled just sufficiently to trigger the heterogeneous nucleation of water, reheated to −2°C and immediately recooled showed just the low enthalpy transitions centered at −30°C and −40°C. The small exotherm centred at about −40°C is commonly seen in lipid

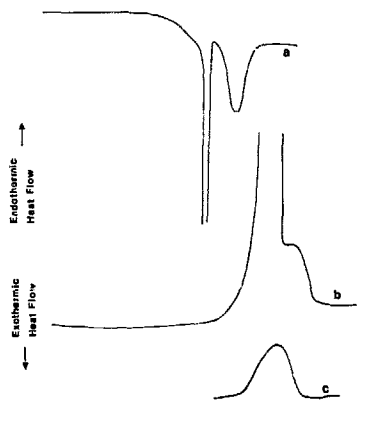

Fig. 2. Typical thermograms of an unsaturated MGDG sample cycled between −50°C and 10°C at a rate of 5 C°/min (a) cooling scan, (b) heating scan and (c) heating scan obtained when the sample was heated from −10°C to prevent ice formation, instead of −50°C.

samples [21] and is almost certainly due to the homogeneous nucleation of isolated pockets of supercooled water. The broad exotherm centred at −30°C in contrast, would be expected to be associated with a lipid transition.

On reheating the sample from −50°C, an exotherm starting at −10°C is first observed. This is, closely followed by a large endotherm at 0°C, corresponding to the melting of ice, and a smaller overlapping endotherm centred at about 8°C, as shown in Fig. 1b. This behaviour was observed in repeated scans and did not appear to vary with time spent at either 20°C or −50°C.

The cooling thermogram is, however, greatly influenced by the temperature to which the sample is heated prior to cooling. If the cooled sample is heated to 10°C rather than 20°C before re-cooling, a thermogram of the type displayed in Fig. 2a is obtained. A new exotherm appears with an onset temperature of about −2°C and a molar enthalpy of approx. 9 kcal/mol. This is followed by the usual ice exotherm at about −15°C. The small broad exotherm centered at −30°C and the small exotherm seen at −40°C are very much reduced under these conditions and often disappear altogether.

The heating thermogram obtained on reheating samples cooled from 10°C also differs from that obtained from samples cooled from higher temperatures (cf. Fig. 1b and Fig. 2b). The exotherm prior to the ice endotherm is no longer present suggesting that the cooling exotherm at about −2°C reflects the occurrence of a transition to a low-temperature phase which can occur in samples heated to less than 12°C but not in those heated to higher temperatures. The exotherm seen in the heating curves of samples cooled from temperatures above 12°C thus appears to reflect a belated occurrence of this transition to this low-temperature phase.

On this basis, the heating endotherm centred at about 8°C should correspond to the transition from the low-temperature phase back to the high-temperature phase that normally exists at temperatures above 12 C. Estimation of the enthalpy of this transition is difficult in thermograms of the type shown in Figs. 1b and 2b because of the overlap of the ice peak. This problem was overcome by making sure that the temperature of the sample did not fall low enough to trigger ice formation, i.e., reheating the sample before the supercooled water present in the sample had a chance to freeze. An example of such a measurement is shown in Fig. 2c. The heating endotherm measured under these conditions has an onset temperature of −2°C and a molar enthalpy value of 9.6 ± 0.5 kcal/mol.

Samples cooled from temperatures above 12°C lacked this new cooling endotherm and yielded thermograms of the type shown in Fig. 1a. If, the samples were cooled to −10°C and reheated before water freezing occurred, the thermograms were completely featureless indicating that the samples had remained in the high-temperature phase through the cooling/heating cycle.

The normal high-temperature phase in saturated and unsaturated MGDG samples is Hex_{II} [8,12]. The low-temperature phase obtained on cooling from the Hex_{II} phase, in saturated samples at least, is L_β. This L_β phase can then undergo an exothermic relaxation on storage to one of two possible crystalline sub-gel phases L_{c1} or L_{c2} [7,9]. The relationship between this phase behaviour and that of the unsaturated lipids as reflected in the thermal data is not immediately obvious.

X-ray diffraction

In order to obtain a clearer idea of the origin of the different transitions seen in the thermal measurements, real-time X-ray diffraction measurements were made under similar conditions to those used in the DSC studies. A series of diffraction patterns obtained on cooling the sample from 20°C to −50°C at a rate of

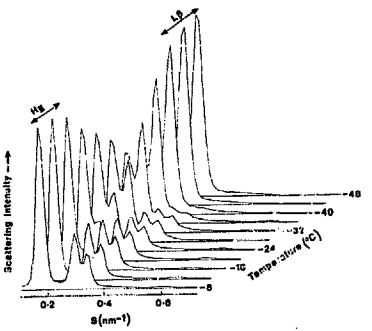

Fig. 3. Selected frames from a series of real-time, narrow-angle X-ray diffraction patterns of unsaturated MGDG measured during a cooling scan from 20°C to −50°C carried out at a cooling rate of 5 C°/min illustrating the conversion of the sample from the Hex_{II} to the L_{β} phase.

5 C°/min is presented in Fig. 3. A very slow transition beginning at around −15°C and continuing to the end of the scan is observed. More detailed diffraction patterns of samples measured at 20°C and −40°C are presented in Fig. 4. Repeat scans were effectively identical suggesting that radiation damage was not a major factor in these measurements.

The diffraction maxima of the sample measured at 20°C, as anticipated, index in a ratio of $1:1/\sqrt{3}:1/\sqrt{4}$ and are characteristic of a Hex_{II} phase with a d-spacing of 5.71 nm. In agreement with the thermal data, a broad transition starting at about −16°C is seen on cooling. The low temperature diffraction pattern, however, is very poorly defined. The narrow-angle region consists of a first order maximum together with some indication of two poorly resolved peaks possibly corresponding to second and third order maxima of a lamellar phase. The d-spacing calculated from the first order maximum is 4.60 nm. Two poorly defined maxima were visible in the wide angle region of the diffraction pattern at 0.38 and 0.36 nm (Fig. 4). These maxima which first appear at −17°C are, for reasons outlined below, attributed to the two stronger of the three diffraction maxima of the hexagonal ice pattern [15]. No obvious wide-angle diffraction peaks of the type normally associated with either the L_{β} or L_c phases of MGDG [7,9] were observed.

A second set of X-ray diffraction patterns were collected as the sample was reheated from −50°C. The narrow-angle region of a selection of these patterns is displayed in Fig 5a. The sample started the heating scan in the same relatively disordered phase seen in the cooling scan. At around −20°C, a shoulder begins to grow on the high d-spacing side of the first-order peak and second- and third-order maxima characteristic of a lamellar phase with a d-spacing of about 5.4 nm start to become visible. Above −10°C, the intensity of this new first-order peak increases rapidly. Shortly afterwards, a new set of diffraction orders begin to appear which by −2°C can be clearly assigned to an Hex_{II} phase. Continued heating leads to a growth of this Hex_{II} phase at the expense of the newly formed-lamellar phase. By the time that the sample reaches 7°C, the Hex_{II} phase is the dominant phase and the d-spacing has swollen to 5.8 nm.

Further evidence of these transitions comes from the corresponding wide-angle data, examples of which are presented in Fig. 5b. At −50°C, the scatter in this region is diffuse apart from the two small peaks at 0.38 and 0.36 nm. This situation continues until at −11°C, the lipid chain order suddenly increases and two new diffraction peaks appear at 0.485 and 0.43 nm. The 0.38 and 0.36 nm maxima disappear abruptly at 0°C confirming that they arise from ice but the 0.485 and

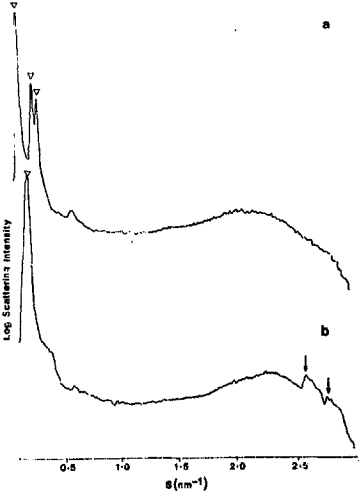

Fig. 4. X-ray diffraction patterns of unsaturated MGDG measured at (a) 20°C and (b) after cooling to −40°C. The arrows in the low-angle region indicate the diffraction maxima used to characterise the phase. Those in the wide-angle indicate the maxima attributed to ice.

0.43 maxima persist until around 6°C when they are replaced by a broad peak centred at 0.46 nm characteristic of fluid chains.

The wide-angle maxima at 0.485 and 0.43 nm clearly reflect the packing of the lipid acyl chains. Similar maxima centred at 0.46 and 0.41 nm are seen in the L_{c1} phase of distearoyl MGDG [11] suggesting that the transitory lamellar phase formed at −10°C is an L_{c1} phase. Freeze-fracture data, discussed below, confirm that the poorly organised precursor phase is also a lamellar phase. In the absence of wide-angle diffraction maxima arising from the lipid chains, assignment of this latter phase is difficult. The obvious candidates are the L_β phase and the L_{c2} phase seen in saturated MGDG samples stored at low temperatures [9,11]. Both of these phases, in saturated MGDG at least, are characterised by smaller d-spacings than the L_{c1} phase and are capable of undergoing exothermic transitions to the L_{c1} phase. The fact that the L_β phase is normally the first gel phase formed on cooling non-bilayer lipids and that the L_c phases, if seen, are usually only seen after storage at low temperatures strongly suggests that the disordered lamellar phase initially formed on cooling MGDG is a partially ordered L_β phase.

A similar set of X-ray diffraction measurements was carried out to determine the origin of the exotherm observed at around −2°C in samples cooled from temperatures below 12°C (Fig. 2a). The resulting patterns are presented in Fig. 6. At 7°C, the sample was in the Hex_{II} phase (d = 5.85 nm, wide-angle diffraction centred at 0.46 nm). At −5°C a transition to a highly ordered lamellar phase took place which was completed by −15°C. The low-temperature phase obtained under these conditions clearly differs from that obtained when the samples are cooled from a starting temperature of 20°C (cf. Figs 3 and 6).

A full diffraction pattern for this phase, collected at −30°C, is presented in Fig. 7. Four orders of diffraction indexing in the ratio of 1:1/2:1/3:1/4 indicate that the phase is lamellar with a repeat spacing of 5.69 nm. The wide-angle region consists of two lipid peaks centred at 0.48 and 0.43 nm and the two ice peaks at about 0.38 and 0.36 nm. The low-temperature phase, in this case, is clearly identical to the transitory lamellar phase formed in the reheating experiments illustrated in Fig. 5 and shows all the characteristics of an L_{c1} phase. The extra reflection at 0.786 nm seen in the central region of the diffraction pattern probably cor-

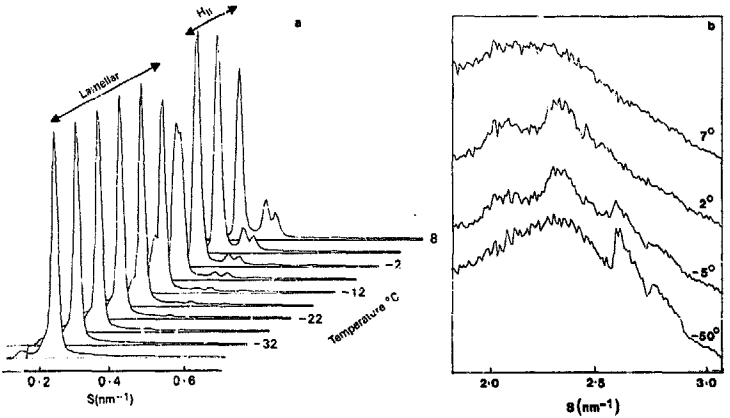

Fig. 5. Selected frames from a series of real-time X-ray diffraction patterns of unsaturated MGDG measured during a heating scan from −50°C to 20°C carried out at a heating rate of 5 C°/min illustrating the conversion of the sample first from the disordered low-temperature gel phase to the L_{c1} phase and then from the L_{c1} to the Hex_{II} phase (a) narrow-angle measurements and (b) wide-angle measurements. The temperatures at which the data was collected are indicated in the figure.

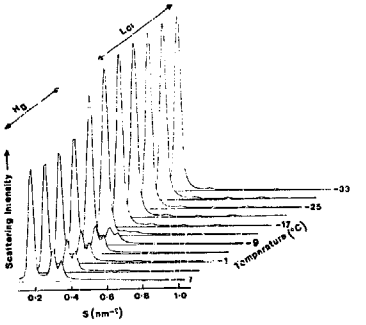

Fig. 6. Selected frames from a series of real-time, narrow-angle X-ray diffraction patterns of unsaturated MGDG measured during a cooling scan from 10°C to −50°C carried out at a cooling rate of 5 C°/min illustrating the direct conversion of the Hex_{II} to the L_{c1} phase in samples retaining a nucleus of L_{c1} phase lipid.

responds to the maximum, attributed to an ordering of the sugar residues of the lipid headgroups, seen at about 0.69 nm in the distearoyl derivative [9].

On-reheating (data not shown) this L_{c1} phase converts directly to Hex_{II}. The transition started at −2°C; the ice peaks disappeared by 1°C and the L_{c1} peaks persisted to 5°C. Again, this matches well with the

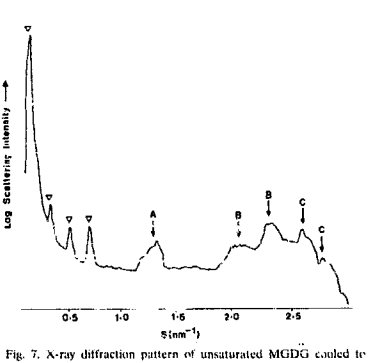

Fig. 7. X-ray diffraction pattern of unsaturated MGDG cooled to −30°C. The sample was pre-cooled to −50°C, heated to 10°C and then re-cooled to the measuring temperature directly before measurement. Arrows indicate the low-angle diffraction maxima used to characterize the lamellar phase. Diffraction maxima indicated by A, B, C are attributed to the sugar headgroups, the lipid chains and ice, respectively.

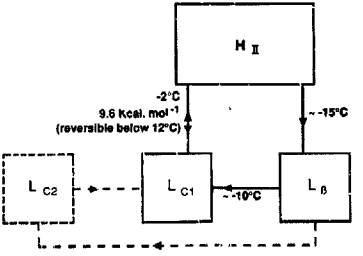

Fig. 8. Diagram illustrating the pattern of phase transitions observed for unsaturated MGDG. Solid lines indicate transitions observed in the DSC. Dashed lines indicate the possible involvement of a second crystalline gel phase (L_{c2}). See text for details.

thermal data displayed in Fig. 2b which showed just the one lipid transition occurring at −2°C. The lack of any exotherm at −10°C reflects the fact that the lipid is already in the L_{c1} phase at low temperatures and that as such no exothermic transition between the L_β and L_{c1} phases occurs on heating.

The difference between the phase behaviour of samples cooled from temperatures below 12°C and those cooled from higher temperatures thus appears to reflect the retention of a small component of lipid in the L_{c1} phase until around 12°C. This is then able to nucleate a $Hex_{II} \rightarrow L_{c1}$ transition on re-cooling the sample. Above 12°C, the $L_{c1} \rightarrow Hex_{II}$ transition goes to completion and this nucleation process then cannot occur.

A diagram illustrating these various transitions is presented in Fig. 8. It closely resembles earlier schemes put forward to account for the phase behaviour of saturated MGDG samples [7,9]. The existence of a second gel crystal form L_{c2} as a possible intermediate on the pathway from L_β to L_{c1} is indicated in the diagram. This is based on the observation that an L_{c2} phase that converts to L_{c1} on heating is formed on low-temperature storage of the L_β phase of saturated MGDG samples [7]. It must be emphasised that no direct evidence for the formation of L_{c2} was obtained in the present experiments.

Freeze-fracture electron microscopy

As a final confirmation of this scheme, the identity of the different phases was examined by freeze-fracture measurements. The heating and cooling regimes used in the DSC and X-ray diffraction measurements were reproduced in the controlled heating/cooling chamber mentioned in Methods, allowing samples to be thermally quenched at different stages in the cycle.

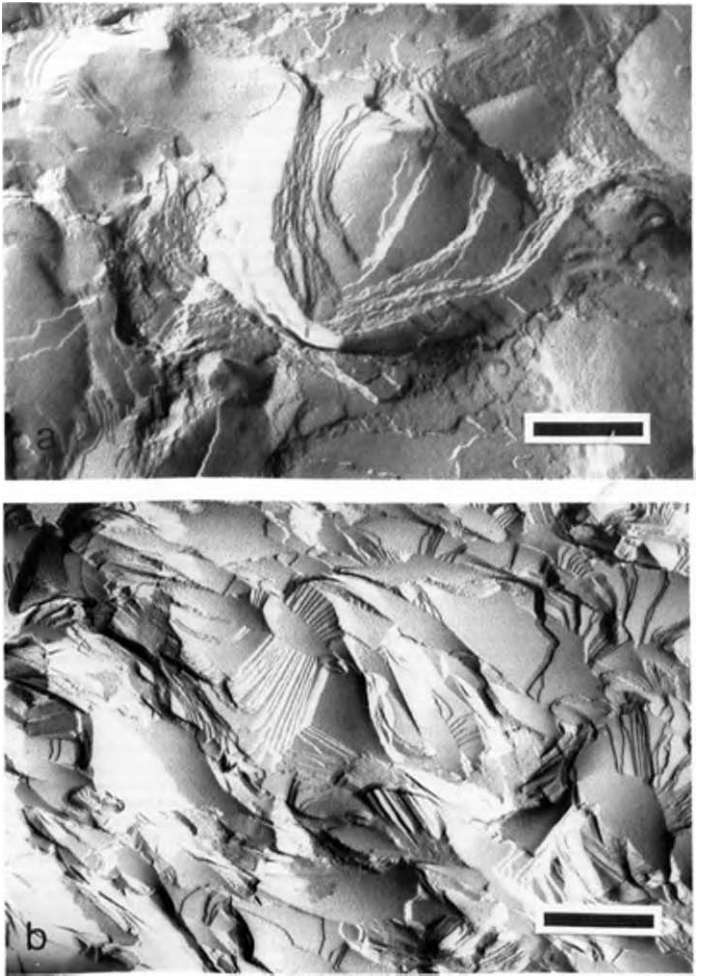

Fig. 9. Freeze-fracture electronmicrographs of samples thermally quenched following different heating/cooling regimes (a) sample cooled from 20°C to −50°C, (b) sample pre-cooled to −50°C, re-heated to 10°C prior to final cooling to −10°C. Scale bars 1 μm.

Samples quenched directly from 20°C were in the Hex_{II} phase as expected (data not shown). Samples cooled from 20°C to −50°C at a rate of 5 C°/min formed liposomal structures indicating that they were in a lamellar phase. However, as illustrated in Fig. 9a, a significant amount of Hex_{II} phase lipid remains indicating that the transition to the lamellar phase does not reach completion. The electronmicrograph presented in Fig. 9b, shows a replica of a sample which has first been cooled to −50°C, allowed to rewarm to 10°C and then recooled to −10°C before thermal quenching. According to the scheme proposed above, the sample should be in the L_{c1} phase. The replica clearly shows that the lipid is in a non-liposomal lamellar phase. The bilayers are arranged in curved multilamellar stacks distributed in a haphazard fashion closely resembling structures previously reported for the L_{c1} phase of saturated MGDG samples [10].

Estimation of size of nucleating L_{c1} fraction

Traces of the diffraction pattern of the L_{c1} phase can be detected up to a temperature of around 8°C in narrow-angle X-ray diffraction measurements of the type shown in Figs. 5a. The proportion of the lipid remaining in the L_{c1} phase is, however, more easily estimated from DSC measurements.

A series of DSC scans were made to determine the enthalpy of the $Hex_{II} \rightarrow L_{c1}$ transition on cooling following an initial pre-heating to different temperatures in the range 6–14°C. The measured enthalpy values, listed in Table I, increase slowly with increasing temperature between 6 and 12°C and then fall abruptly to zero. The true enthalpy of this transition is taken to be 9.6 kcal/mol, the value obtained from heating scans of the type shown in Fig. 2c. The reductions in enthalpy of the transition on cooling are attributed to the presence of lipid that has remained in the L_{c1} phase and as such does not contribute to the subsequent $Hex_{II} \rightarrow L_{c1}$ transition. The proportion of lipid remaining in the L_{c1} phase at the different starting temperatures (i.e., the proportion of nucleating L_{c1} in the samples) is taken to equal the proportional reduction of the measured enthalpy with respect to the value calculated from a full heating curve. This varies from 22% at 6°C down to 3% at 12°C. These values were independent of the time spent at the given temperatures and probably reflect the presence of small amounts of more-saturated molecular species that have rather higher phase transitions than the bulk of the sample.

TABLE I

Estimates of the proportion of lipid remaining in the nucleating L_c phase of samples preheated to different temperatures

Upper temperature prior to cooling (°C)	Enthalpy of Hex_{II}–L_c transition (kcal/mol)	Proportion of lipid remaining in L_c phase (%)
6	7.5 ± 0.5	22
8	8.2 ± 0.5	14
10	9.1 ± 0.5	5
12	9.3 ± 0.5	3
14	0.0	0

Discussion

Unsaturated MGDG isolated from the leaves of the broad bean *Vicia faba* consists predominantly of the dilinolenoyl (di-18:3) derivative of the lipid [12,13]. Its phase behaviour, after due allowance is made for the observational difficulties associated with the fact that most of the important transitions take place at temperatures below the freezing point of water, is summarised in Fig. 8. This behaviour is very similar to that previously reported for the fully saturated distearoyl (di-18:0) derivative [7,9]. In both cases, the high-temperature phase is the Hex_{II} phase and this converts to an L_β phase which subsequently undergoes an exothermic reorganisation to an L_c phase(s). X-ray diffraction measurements revealed the formation of an L_{c1} phase directly equivalent to that seen for saturated lipids. No direct evidence was found for the formation of the corresponding L_{c2} phase observed on low-temperature storage of the saturated lipid. This may, however, simply reflect the difficulties involved in performing the appropriate long-term storage experiments.

The major difference between the unsaturated and saturated lipids is that the $Hex_{II} \rightarrow L_\beta$ transition in the unsaturated lipid appears to be both much broader and of a much lower enthalpy than the corresponding transition in saturated lipids. In our experiments, the $Hex_{II} \rightarrow L_\beta$ transition starts at about −15°C and appears to be incomplete, as judged by freeze-fracture electron microscopy, even at temperatures as low as −50°C. There is also no sign of the sharp wide-angle diffraction maximum at about 0.42 nm normally associated with the hexagonal packing of the acyl chains in the L_β phase.

There are a number of well-documented studies of low-temperature gel to liquid-crystal phase transitions occurring in phosphatidylcholines in which one, or both, the acyl chains are polyunsaturated [16–24]. A common feature of these reports is that the transitions, like those reported here for polyunsaturated MGDG, are characterised by broad transitions with low enthalpies. These effects are particularly marked in the case of phosphatidylcholines containing two polyunsaturated residues where the transitions often span 20–30°C and have molar enthalpies of only 1–2 kcal/mol [23,24].

Keough and Kariel [23] have suggested that this broadening of the transitions might reflect the formation of very disordered gel phases, or the involvement

of intermediate states in the transitions, in lipids containing highly unsaturated acyl chains. Measurements performed on a series of phosphatidylcholines containing stearate (18:0) or eicosoate (20:0) in the *sn*-1 position and a series of corresponding acids with increasing numbers of *cis* double bonds in the *sn*-2 position tend to support the view that acyl chain packing efficiency decreases with the inclusion of increased numbers of double bonds [21,22]. In the case of MGDG, our X-ray diffraction measurements show no evidence of transitional phases but the polyunsaturated chains are clearly extremely disorganised in the L_β phase. Regular chain packing is, however, reimposed on conversion to the L_{c1} phase (Fig. 5b).

The possible effect of the presence of ice on lipid phase transitions has received little attention. The occurrence of lipid phase transitions in frozen systems presupposes the existence of sufficient unfrozen water to allow the spatial re-organisation associated with such transitions to take place. The fact that concentrated lipid dispersions normally contain appreciable amounts of unfrozen water at temperatures well below the freezing point of their bulk water was first pointed out by Chapman et al. [14]. Bronshtevn and Steponkus [25] have recently re-investigated the freezing of water in concentrated lipid suspensions. Careful DSC measurements performed by these authors indicate that unfrozen water can persist in such suspensions to temperatures below −80°C. They also demonstrated that the melting of ice in such lipid samples commences at temperatures as low as −50°C.

Bilayer to non-bilayer transitions of the type ocurring in MGDG involve considerably more structural re-organisation of the lipid than occurs in the gel to liquid-crystal transitions exhibited by bilayer forming lipids such as the phosphatidylcholines. The possiblity that some of the broadening effects seen at low temperatures seen in the case of MGDG are related to the presence of ice thus cannot be completely excluded. The non-bilayer to bilayer transition occurring in MGDG coincides with the gel to liquid-crystal transition, i.e., it is a $Hex_{II} \rightarrow L_\beta$ transition. The effect of double bonds on the less-energetic transition from $Hex_{II} \rightarrow L_\alpha$, commonly seen in lipids such as the phosphatidylethanolamines, has yet to be examined.

Acknowledgements

The help and advice of Wim Bras of the SERC Daresbury, Synchrotron Facility, of Tony Brain of the Electron Microscopy Unit of King's College and of our colleagues Peter Quinn and Leonard Lis are gratefully acknowledged as is the support of the Science and Engineering Research Council.

References

1 Mannock, D.A., Lewis, R.N.A.H., Sen, A. and McElhaney, R.N. (1988) Biochemistry, 27, 6852–6859
2 Mannock, D.A., Lewis, R.N.A.H. and McElhaney, R.N. (1990) Biochemistry 29, 7789–7799.
3 Sen, A., Hui, S.-W., Mannock, D.A., Lewis, R.N.A.H. and McElhaney, R.N. (1990) Biochemistry, 29, 7796–7799.
4 Lewis, R.N.A.H., Mannock, D.A., McElhaney, R.N., Wong, P.T.T. and Mantsch, H.H. (1990) Biochemistry, 29, 8933–8943.
5 Quinn, P.J. and Williams, W.P. (1983) Biochim. Biophys. Acta 737, 223–266.
6 Shipley, G.G., Green, J.P. and Nicholls, B.W. (1973) Biochim. Biophys. Acta, 311, 531–544.
7 Sen, A., Mannock, D.A., Collins, D.J., Quinn, P.J. and Williams, W.P. (1983) Proc. R. Soc. Lond., B218, 349–364.
8 Sen, A., Williams, W.P. and Quinn, P.J. (1981) Biochim. Biophys. Acta, 663, 380–389.
9 Lis, L.J. and Quinn, P.J. (1986) Biochim. Biophys. Acta, 862, 81–86.
10 Mannock, D.A., Brain, A.P.R. and Williams, W.P. (1985) Biochim. Biophys. Acta 817, 289–298.
11 Mannock, D.A., Brain, A.P.R. and Williams, W.P. (1985) Biochim. Biophys. Acta 821, 153–164.
12 Gounaris, K., Sen, A., Brain, A.P.R., Quinn, P.J. and Williams, W.P. (1983) Biochim. Biophys. Acta, 728, 129–139.
13 Gounaris, K., Mannock, D.A., Sen, A., Brain, A.P.R., Williams, W.P. and Quinn, P.J. (1983) Biochim. Biophys. Acta 732, 229–242.
14 Chapman, D., Williams, R.M. and Ladbooke, B.D. (1967) Chem. Phys. Lipids 1, 445–475.
15 Dowell, L.G., Moline, S.W. and Rinfret, A.P. (1962) Biochim. Biophys. Acta 59, 229–242.
16 Philips, M.C., Williams, R.M. and Chapman, D. (1969) Chem. Phys. Lipids 3, 234–244.
17 Philips, M.C., Ladbroke, B.D. and Chapman, D. (1970) Biochim. Biophys. Acta 196, 35–44.
18 Philips, M.C., Hauser, H. and Pattauf, P. (1972) Chem. Phys. Lipids 8, 127–133.
19 Barton, P.G. and Gunstone, F.D. (1975) J. Biol. Chem. 250, 4470–4476.
20 Silvius, J.R. and McElhaney, R.N. (1979) Chem. Phys. Lipids 25, 125–134.
21 Coolbear, K.P., Berde, C.B. and Keough, K.M.W. (1983) Biochemistry 22, 1466–1473.
22 Keough, K.M.W., Giffin, B. and Kariel, N. (1987) Biochim. Biophys. Acta 902, 1–10.
23 Keough, K.M.W. and Kariel, N. (1987) Biochim. Biophys. Acta 902, 11–18.
24 Kariel, N., Davidson, E. and Keough, K.M.W. (1991) Biochim. Biophys. Acta 1062, 70–76.
25 Bronshtevn, V.L. and Steponkus, P.L. (1991) Cryobiology 28, A56.